Title: Protected area planning to conserve biodiversity in an uncertain world

Authors: Richard Schuster [1,2*], Rachel Buxton[1], Jeffrey O. Hanson[1], Allison D. Binley[1], Jeremy Pittman[3], Vivitskaia Tulloch[4], Frank A. La Sorte[5], Patrick R. Roehrdanz[6], Peter H. Verburg[7], Amanda D. Rodewald[5,8], Scott Wilson[1,9], Hugh P. Possingham[10], Joseph R. Bennett[1]

Affiliations:

[1] Department of Biology, 1125 Colonel By Drive, Carleton University, Ottawa ON, K1S 5B6 Canada.

[2] Nature Conservancy of Canada, 245 Eglinton Ave East, Suite 410, Toronto, Ontario, M4P 3J1, Canada.

[3] School of Planning, University of Waterloo, 200 University Ave W, Waterloo, ON, N2T 3G1, Canada

[4] Conservation Decisions Lab, Department of Forest and Conservation Sciences, 2424 Main Mall, Vancouver, BC V6T 1Z4, Canada.

[5] Cornell Lab of Ornithology, Cornell University, Ithaca, NY 14850, USA

[6] Conservation International, 2100 Crystal Drive #600, Arlington, VA 22202, USA

[7] Institute for Environmental Studies, VU University Amsterdam, Amsterdam, The Netherlands

[8] Department of Natural Resources and the Environment, Cornell University, Ithaca, NY 14853, USA.

[9] Wildlife Research Division, Environment and Climate Change Canada, 1125 Colonel By Drive, Ottawa, Ontario, Canada, K1S 5B6

[10] Centre for Biodiversity and Conservation Science, University of Queensland, St Lucia, Queensland 4067, Australia

*Corresponding author. Email: richard.schuster@glel.carleton.ca

Abstract: Despite being key instruments for conservation, protected areas are vulnerable to risks associated with weak governance, land use intensification, and climate change. We developed a hierarchical spatial optimization routine to maximize protection for all known terrestrial vertebrate species and found that expanding the global protected area system while explicitly accounting for such risks requires small (1.6%) increases in land area relative to plans that do not consider risk. Among the three risk categories, the risk of governance failure drove the biggest changes in priority areas for protection. Conserving wide-ranging species required countries with relatively strong governance to protect more land when bordering nations with comparatively weak governance. Our results underscore the need for cross-jurisdictional coordination and demonstrate how risk can be efficiently incorporated into conservation planning.

One-Sentence Summary:

To safeguard biodiversity, protected areas should account for risk related to climate and land use change, and governance.

Main Text: Protecting habitat is one of the best strategies for stemming the alarming decline of biodiversity (*1*). As such, international agreements to protect increasing amounts of land area have become cornerstones of efforts to protect biodiversity *(2,3*). Most current approaches for identifying important areas to protect rely upon estimations of the conservation value of the land for biodiversity (*2-5*). Seldom articulated in such plans is the tacit assumption that protection will be enforced, effective, and permanent; yet many protected areas are subject to risks caused by weak governance, land use intensification, and climate change. For example, political instability and corruption can reduce protected area effectiveness (*6,7*). Likewise, high deforestation rates can increase the risk of degazetting protected areas and failing to meet protection goals (*8,9*); and the increasing frequency and intensity of extreme weather events can threaten the persistence of species populations within protected areas (*10*). Thus, effective use of limited conservation resources requires planning for investment in protected areas that accounts for these risks (*11*,*12*). Here we demonstrate how accounting for governance, land use, and climate risks influences decisions for establishing protected areas at a global scale and can ultimately improve the resilience of protected areas and the species they support (*13*,*14*).

We considered the following three broad categories of risk, which we defined as factors likely to diminish the long-term effectiveness of protected areas: (i) governance, (ii) land use, and (iii) climate. For governance risk, we used a national-scale metric that combines six governance indicators from the World Bank (*15*): accountability, political stability, government effectiveness, regulatory quality, rule of law, and control of corruption (Fig. S1). For land use risk, we estimated the average change in biodiversity per land use category using methods (*16*) that model the risk of biodiversity loss for land systems due to land use type and intensity (Fig. S2). For climate risk, we used predicted climate velocity, which is the horizontal velocity along the Earth's surface a hypothetical species would need to maintain a constant temperature as climate changes (Fig. S3) (*17*). In addition, to illustrate the effect of using alternative risk measures, we use the duration of extreme heat events, calculated using a probabilistic framework that estimates the novelty of temperatures relative to historical year-to-year variation from 1979 to 2019, identifying areas where extreme heat events are likely to have the most significant effects on biodiversity (*18*) (see Supplementary Material for details). The metrics we chose correspond to key aspects of risk in protected area allocation. However, they represent only a few options among the many that agencies may choose to use. The approach we propose is flexible and can easily incorporate additional or alternative risk metrics (*19*).

We considered the influence of risk categories on allocating protection decisions at a global scale in suitable habitat for all 29,350 vertebrate species from the IUCN Red List of Threatened Species (*20*) using a multi-objective optimization approach. To incorporate risk categories, we built on a classical problem formulation from the systematic conservation planning literature – the minimum set problem - where the objective is to reach species distribution protection targets while accounting for one constraint such as land cost or area (*21-23*). We expanded this approach to include multiple objectives accounting for varying risk in the problem formulation, by treating each risk layer as a separate objective in the problem formulation (*24*). We used a hierarchical approach that assigns a priority to each objective and optimizes for the objectives in decreasing priority order. At each step, the approach finds the best solution for the current objective, but only from among those that would not degrade the solution quality for higher-priority objectives.

In total 16 planning scenarios were created, such that solutions accounted for all possible combinations of risk categories within each hierarchical level (Table S1). We then compared these risk-based solutions to those produced with a null scenario that adopted the traditional areaminimizing approach to optimization without considering risk (*25*). Because our scenarios aimed to build upon the current protected area portfolio globally, we incorporated current protected areas into our solutions. For each scenario we set species-based targets based on percentages of suitable habitat protected (*26*). Specifically, we obtained suitable habitat maps (*27*), and set target percentages for each species, from 100% for species with less than 1,000 km^2 of suitable habitat to 10% for those with greater than 250,000 km^2 of suitable habitat, and linearly interpolated on a log-linear scale between these thresholds (*26*).

Surprisingly, scenarios that incorporated combinations of the three risk categories increased the priority area by only 1.6% on average (0.08 – 2.52%) compared to the null scenario for protecting species' suitable habitat. Thus, accounting for risks will require relatively little additional protected area compared to the potential gains from selecting a more resilient conservation network (Fig. 1). When only looking at scenarios that included one risk factor, climate-change risk based on climate velocity required the greatest increase in global protected area, compared to scenarios only including governance or land use intensification risks (Table S1).

We found that protected areas identified across scenarios overlapped spatially, with the same 11.5 million km^2 (7.8% of global land area) being prioritized for expansion of the current protected area system in at least eleven scenarios and 8.5 million km^2 (5.8% of global land area) in all 15 risk scenarios (Fig. 2). These "no regrets" areas provide examples of places that should be immediate priorities for international agencies aiming to maximize the resilience of protected area networks, as they are robust to assumptions about the relative importance of risk factors. Example countries that have contiguous areas of high overlap among different scenarios are Canada, Kenya and Peru (Fig. S4). There was considerable overlap among the priorities across scenarios within Conservation International's global biodiversity hotspots (*28*), but many high overlap areas lie either outside of (53.3%) or in small areas within hotspots (Fig. S5).

There were some important shifts in locations identified as high priority for protection among risk scenarios (Fig. 3; Table S2), with the largest shift being for the risk of weak governance (Fig. S6). Compared to null scenarios, those considering governance risk required protection of greater land area, even for countries with relatively effective governance. This was especially true for protecting wide-ranging species and when neighboring countries had weak governance. For example, many vertebrate species ranges span northeastern Russia and Finland, one of the most iconic being caribou (*Rangifer tarandus*), which has an IUCN conservation status of vulnerable. Because Russia has low scores for 'voice and accountability, rule of law, and control of corruption' (Table S3), whereas Finland has relatively high governance scores, the scenarios including governance pressures led to a selection of 36.4% of Finland's land area compared to the null scenario with 16.2% (Fig. 4).

Land use and climate change also influenced variation in priority locations for protection compared to the null scenario. For example, large areas of Sierra Leone are experiencing high risk of biodiversity loss due to expanding intensive agricultural land use practices (Fig. S2), whereas this same risk is lower in neighboring Liberia. The scenario including land use risk selected 32.1% of the land area in Liberia compared to 22.5% in the null scenario (Fig. 4). Large areas of Hungary and Serbia have high predicted climate velocity (Fig. S3), whereas most of nearby Kosovo has lower predicted climate velocity. Scenarios including climate impact risk selected 20.4% of Kosovo's land area compared to the null scenario with 10.2% (Fig. 4). Including the risk metric predicting frequency of extreme events (*18*) (Fig. S7 – S9) resulted in different priority areas in some cases. For example, large areas of Libya, which is experiencing fewer extreme heat events than neighboring countries, were prioritized in this scenario and not in the null scenario. This difference between climate risk scenarios highlights the need for agencies to carefully consider their choices of risk metrics and suggests that smaller-scale planning exercises should choose metrics that are most relevant for each region.

Overall, our results emphasize the importance of coordinating initiatives to plan conservation across jurisdictions (*29*) and identifying countries where collaborative opportunities promote resilient protected area systems. To illustrate this point, we consider the great green macaw (*Ara ambiguus*), with <2500 individuals remaining (*30*) and a range that stretches from southern Honduras to western Colombia. Because great green macaw habitat spans several countries differing in governance, land use, and climate risk, coordinated efforts among countries will be necessary for the species to persist in the future. Such cooperative governance frameworks (*31*) are especially important for countries supporting wide-ranging species that are expected to be impacted by climate, land use, and governance risk across borders (Fig. 3). These governance frameworks, both within and among countries, would need to be developed in an environmentally just and equitable way to deliver benefits to biodiversity and local communities (*32*).

In contrast, few priorities changed - and protection needs remained high - for countries with high rates of endemism, even amid high risk from climate change, land use, and weak governance. Moreover, some countries with a large proportion of their land already protected, such as Brazil, which has protected 30.3% of its land area, had lower differences between scenarios that incorporate risk and the null scenario, despite having high climate, land use, and governance risk. This highlights the importance of further considering the effectiveness of existing protected areas in planning analyses, in tropical areas where cropland conversion in protected areas has increased to similar rates outside protected areas (*33*).

Previous work has incorporated individual risk factors analogous to those we used, including governance (*34*,*35*), climate change (*36*) and land use change (*37*,*38*) demonstrating the importance of each type of risk in protected area planning. Our results similarly demonstrate that protected area expansion decisions can be profoundly influenced by all three risk factors combined yet show that relatively little additional protected area is required to account for these risks. Our flexible framework and methods can allow conservation agencies to set their own priorities from local to global scales and incorporate different metrics to assess the relevance of different forms and levels of risk.

The conservation community has traditionally neglected to estimate how future changes in climate (*39*), land use (*38*), and socio-economic conditions might compromise the effectiveness of protected areas. Yet, as we work towards an ambitious new plan to curb biodiversity loss (*3*) in a rapidly changing world, we show that incorporating future risk has profound implications for the spatial distribution of protected areas. The risk of weak governance was particularly influential. Surprisingly, incorporating risk into decision-making adds <2% to the total global area required to meet biodiversity targets. Thus, accounting for risk comes at limited extra cost which is likely outweighed by increased likelihood of achieving global biodiversity targets. Our results also emphasize the importance of cross-jurisdictional conservation initiatives, especially in adjacent countries sharing wide-ranging species where risk varies considerably from country to country. Considering risk in conservation decision-making will result in more resilient and effective conservation plans into the future to help safeguard our planet's biodiversity in the face of the current extinction crisis.

References and Notes

1. J. E. Watson, N. Dudley, D. B. Segan, M. Hockings, The performance and potential of protected areas. *Nature* **515**, 67–73 (2014).

2. CBD (Convention on Biological Diversity), Aichi Biodiversity Targets. https://www.cbd.int/sp/targets/ (2020).

3. CBD (Convention on Biological Diversity), Zero draft of the post-2020 global biodiversity framework. Available at https://www.cbd.int/doc/c/efb0/1f84/a892b98d2982a829962b6371/wg2020-02-03-en.pdf (2020).

4. T. M. Brooks, R. A. Mittermeier, G. A. B. da Fonseca, J. Gerlach, M. Hoffmann, J. F. Lamoreux, C. G. Mittermeier, J. D. Pilgrim, A. S. L. Rodrigues, Global biodiversity conservation priorities. *Science* **313**, 58–61 (2006).

5. O. Venter, R. A. Fuller, D. B. Segan, J. Carwardine, T. Brooks, S. H. Butchart, M. Di Marco, T. Iwamura, L. Joseph, D. O'Grady, H. P. Possingham, Targeting Global Protected Area Expansion for Imperiled Biodiversity. *PLOS Biol.* **12**, e1001891 (2014).

6. K. Schulze, K. Knights, L. Coad, J. Geldmann, F. Leverington, A. Eassom, M. Marr, S. H. M. Butchart, M. Hockings, N. D. Burgess, An assessment of threats to terrestrial protected areas. *Conserv. Lett.* **11**, e12435 (2018).

7. E. Hammill, A. I. T. Tulloch, H. P. Possingham, N. Strange, K. A. Wilson, Factoring attitudes towards armed conflict risk into selection of protected areas for conservation. *Nat. Commun.* **7**, 11042 (2016).

8. A. T. Tesfaw, A. Pfaff, R. E. G. Kroner, S. Qin, R. Medeiros, M. B. Mascia, Land-use and land-cover change shape the sustainability and impacts of protected areas. *Proc. Natl. Acad. Sci.* **115**, 2084–2089 (2018).

9. R. E. G Kroner, S. Qin, C. N. Cook, R. Krithivasan, S. M. Pack, O. D. Bonilla, K. A. Cort-Kansinally, B. Coutinho, M. Feng, M.I.M. Garcia, Y. He, The uncertain future of protected lands and waters. *Science* 364, no. 6443 (2019): 881-886.

10. S. L. Maxwell, N. Butt, M. Maron, C. A. McAlpine, S. Chapman, A. Ullmann, D. B. Segan, J. E. M. Watson, Conservation implications of ecological responses to extreme weather and climate events. *Divers. Distrib.* **25**, 613–625 (2019).

11. M. F. McBride, K. A. Wilson, M. Bode, H. P. Possingham, Incorporating the effects of socioeconomic uncertainty into priority setting for conservation investment. *Conserv. Biol.* **21**, 1463–1474 (2007).

12. D. Alagador, J. O. Cerdeira, M. B. Araújo, Shifting protected areas: scheduling spatial priorities under climate change. *J. Appl. Ecol.* **51**, 703–713 (2014).

13. J. McGowan, R. Weary, L. Carriere, E. T. Game, J. L. Smith, M. Garvey, H. P. Possingham, Prioritizing debt conversion opportunities for marine conservation. *Conserv. Biol.* **34**, 1065–1075 (2020).

14. C. D. Kuempel, K. R. Jones, J. E. M. Watson, H. P. Possingham, Quantifying biases in marine-protected-area placement relative to abatable threats. *Conserv. Biol.* **33**, 1350–1359 (2019).

15. D. Kaufmann, A. Kraay, M. Mastruzzi, The worldwide governance indicators: methodology and analytical issues. *Hague J. Rule Law* **3**, 220–246 (2011).

16. L. Kehoe, A. Romero-Muñoz, E. Polaina, L. Estes, H. Kreft, T. Kuemmerle, Biodiversity at risk under future cropland expansion and intensification. *Nat. Ecol. Evol.* **1**, 1129–1135 (2017).

17. S. R. Loarie, P. B. Duffy, H. Hamilton, G. P. Asner, C. B. Field, D. D. Ackerly, The velocity of climate change. *Nature* **462**, 1052-1055 (2009).

18. F.A. La Sorte, A. Johnston, T. R. Ault, Global trends in the frequency and duration of temperature extremes. *Clim. Change* **166,** 1-14 (2021).

19. R. A. Garcia, M. Cabeza, C. Rahbek, M. B. Araújo, Multiple dimensions of climate change and their implications for biodiversity. *Science* **344**, 1247579 (2014).

20. IUCN. The IUCN red list of threatened species. version 1.18. Available at https://www.iucnredlist.org/ (2019).

21. C. R. Margules, R. L. Pressey, Systematic conservation planning. *Nature* **405**, 243–53 (2000).

22. A. Moilanen, K. Wilson, H. Possingham, *Spatial conservation prioritization: quantitative methods and computational tools* (Oxford University Press, 2009).

23. I. R. Ball, H. P. Possingham, M. E. Watts, "Marxan and relatives: Software for spatial conservation prioritization" in *Spatial conservation prioritisation: Quantitative methods and computational tools* (Oxford University Press, 2009), pp. 185–195.

24. K. Deb, "Multi-objective optimization" in *Search methodologies* (Springer, 2014), pp. 403–449.

25. IUCN, Post-2020 global biodiversity framework. Available at https://www.iucn.org/theme/global-policy/our-work/convention-biological-diversity-cbd/post-2020-global-biodiversity-framework (2018).

26. J. O. Hanson, J. R. Rhodes, S. H. M. Butchart, G. M. Buchanan, C. Rondinini, G. F. Ficetola, R. A. Fuller, Global conservation of species' niches. *Nature* **580**, 232–234 (2020).

27. T. M. Brooks, S. L. Pimm, H. R. Akçakaya, G. M. Buchanan, S. H. M. Butchart, W. Foden, C. Hilton-Taylor, M. Hoffmann, C. N. Jenkins, L. Joppa, B. V. Li, V. Menon, N. Ocampa-Peñuela, C. Rondinini, Measuring terrestrial area of habitat (AOH) and its utility for the IUCN red list. *Trends Ecol. Evol.* **34**, 977–986 (2019).

28. N. Myers, R. A. Mittermeier, C. G. Mittermeier, G. A. B. da Fonseca, J. Kent, Biodiversity hotspots for conservation priorities. *Nature* **403**, 853–858 (2000).

29. M. Dallimer, N. Strange, Why socio-political borders and boundaries matter in conservation. *Trends Ecol. Evol.* **30**, 132–139 (2015).

30. Bird Life International, Ara ambiguus. The IUCN red list of threatened species 2020: e.T22685553A172908289. Available at https://dx.doi.org/10.2305/IUCN.UK.2020-3.RLTS.T22685553A172908289.en (2016).

31. R. L. Miller, H. Marsh, C. Benham, M. A. Hamann, Framework for improving the cross-jurisdictional governance of a marine migratory species. *Conserv. Sci. Pract.* **1**, e58 (2019).

32. A. Martin, S. McGuire, S. Sullivan, Global environmental justice and biodiversity conservation. *Geogr. J.* **179**, 122–131 (2013).

33. J. Geldmann, A. Manica, N. D. Burgess, L. Coad, A. Balmford, A global-level assessment of the effectiveness of protected areas at resisting anthropogenic pressures. *Proc. Natl. Acad. Sci.* **116**, 23209–23215 (2019).

34. M. B. Mascia, S. Pailler, Protected area downgrading, downsizing, and degazettement (PADDD) and its conservation implications. *Conserv. Lett.* **4**, 9–20 (2011).

35. J. F. Eklund, M. D. M. Cabeza-Jaimejuan, Quality of governance and effectiveness of protected areas: crucial concepts for conservation planning. *Ann. N. Y. Acad. Sci.* **1399**, 27–41(2017).

36. S. Hoffmann, S. D. Irl, C. Beierkuhnlein, Predicted climate shifts within terrestrial protected areas worldwide. *Nat. Commun.* **10**, 1–10 (2019).

37. F. M. Pouzols, T. Toivonen, E. Di Minin, A. S. Kukkala, P. Kullberg, J. Kuusterä, J. Lehtomäki, H. Tenkanen, P. H. Verburg, A. Moilanen, Global protected area expansion is compromised by projected land-use and parochialism. *Nature* **516**, 383–386 (2014).

38. E. Di Minin, R. Slotow, L. T. Hunter, F. M. Pouzols, T. Toivonen, P. H. Verburg, N. Leader-Williams, L. Petracca, A. Moilanen, Global priorities for national carnivore conservation under land use change. *Sci. Rep.* **6**, 23814 (2016).

39. L. T. Kelly, K. M. Giljohann, A. Duane, N. Aquilué, S. Archibald, E. Batllori, A. F. Bennett, S. T. Buckland, Q. Canelles, M. F. Clarke, M. J. Fortin, Fire and biodiversity in the Anthropocene. *Science* **370**, 6519 (2020).

40. J. A. Hartigan, M. A. Wong, Algorithm AS 136: A K-Means Clustering Algorithm. *J. R. Stat. Soc. Ser. C Appl. Stat.* **28**, 100–108 (1979).

41. S. H. M. Butchart, M. Clarke, R. J. Smith, R. E. Sykes, J. P. Scharlemann, M. Harfoot, G. M. Buchanan, A. Angulo, A. Balmford, B. Bertzky, T. M. Brooks, Shortfalls and solutions for meeting national and global conservation area targets. *Conserv. Lett.* **8**, 329–337 (2015).

42. C. A. Runge, J. E. M Watson, S. H. M. Butchart, J. O. Hanson, H. P. Possingham, R. A. Fuller. Protected areas and global conservation of migratory birds. *Science* **350**, 1255–1258 (2015).

43. A. S. L. Rodrigues, H. R. Akcakaya, S. J. Andelman, M. I. Bakarr, L. Boitani, T. M. Brooks, J. S. Chanson, L. D. Fishpool, G. A. da Fonseca, K. J. Gaston, M. Hoffmann, Global gap analysis: priority regions for expanding the global protected-area network. *Bioscience* **54**, 1092–1100 (2004).

44. IUCN Red List, UNEP-WCMC, Species Range Polygons ver . Available at https://www.iucnredlist.org/resources/other-spatial-downloads. Downloaded 2020-06-01 (2020).

45. Bird Life International, Spatial Data Zone – Birds of the World Species Distribution Data. Available at http://datazone.birdlife.org/species/requestdis. Downloaded 2020-6-1 (2020).

46. L. Santini, S. H. M. Butchart, C. Rondinini, A. Benítez-López, J. P. Hilbers, A. M. Schipper, M. Cengic, J. A. Tobias, M. A. J. Huijbregts, Applying habitat and population-density models to land-cover time series to inform IUCN red list assessments. *Conserv. Biol.* **33**, 1084–1093 (2019).

47. S. E. Fick, R. J. Hijmans, WorldClim 2: new 1-km spatial resolution climate surfaces for global land areas. *Int. J. Climatol.* **37**, 4302–4315.

48. Global administrative areas. GADM database of global administrative areas, version 3.4 Available at http://gadm.org/. Downloaded 2019-10-31 (2018).

49. UNEP-WCWC, IUCN, Protected planet: the world database on protected areas. Available at https://www.protectedplanet.net. Downloaded 2019-11-07 (2019).

50. UNEP-WCWC, IUCN, Protected planet: Calculating protected area coverage. Available at https://www.protectedplanet.net/c/calculating-protected-area-coverage (2021).

51. K. L. Coetzer, E. T. Witkowski, B. F. Erasmus, Reviewing biosphere reserves globally: effective conservation action or bureaucratic label? *Biol. Rev.* **89**, 82–104 (2014).

52. M. D. Barnes, I. D. Craigie, L. B. Harrison, J. Geldmann, B. Collen, S. Whitmee, A. Balmford, N. D. Burgess, T. Brooks, M. Hockings, S. Woodley, Wildlife population trends in protected areas predicted by national socio-economic metrics and body size. *Nat. Commun.* **7**, 12747 (2016).

53. Z. Baynham-Herd, T. Amano, W. J. Sutherland, P. F. Donald, Governance explains variation in national responses to the biodiversity crisis. *Environ. Conserv.* **45**, 407–418 (2018).

54. S. van Asselen, P. H. Verburg, A Land System representation for global assessments and land-use modeling. *Glob. Change Biol.* **18**, 3125–3148 (2012).

55. L. N. Hudson, T. Newbold, S. Contu, S. L. Hill, I. Lysenko, A. De Palma, H. R. Phillips, R. A. Senior, D. J. Bennett, H. Booth, A. Choimes, D. L. Correia, J. Day, S. Echeverría-Londoño, M. Garon, M. L. Harrison, D. J. Ingram, M. Jung, V. Kemp, L. Kirkpatrick, C. D. Martin, Y. Pan, H. J. White, J. Aben, S. Abrahamczyk, G. B. Adum, V. Aguilar-Barquero, M. A. Aizen, M. Ancrenaz, E. Arbeláez-Cortés, I. Armbrecht, B. Azhar, A. B. Azpiroz, L. Baeten, A. Báldi, J. E. Banks, J. Barlow, P. Batáry, A. J. Bates, E. M. Bayne, P. Beja, Å. Berg, N. J. Berry, J. E. Bicknell, J. H. Bihn, K. Böhning-Gaese, T. Boekhout, C. Boutin, J. Bouyer, F. Q. Brearley, I. Brito, J. Brunet, G. Buczkowski, E. Buscardo, J. Cabra-García, M. Calviño-Cancela, S. A. Cameron, E. M. Cancello, T. F. Carrijo, A. L. Carvalho, H. Castro, A. A. Castro-Luna, R. Cerda, A. Cerezo, M. Chauvat, F. M. Clarke, D. F. Cleary, S. P. Connop, B. D'Aniello, P. G. da Silva, B. Darvill, J. Dauber, A. Dejean, T. Diekötter, Y. Dominguez-Haydar, C. F. Dormann, B. Dumont, S. G. Dures, M. Dynesius, L. Edenius, Z. Elek, M. H. Entling, N. Farwig, T. M. Fayle, A. Felicioli, A. M. Felton, G. F. Ficetola, B. K. Filgueiras, S. J. Fonte, L. H. Fraser, D. Fukuda, D. Furlani, J. U. Ganzhorn, J. G. Garden, C. Gheler-Costa, P. Giordani, S. Giordano, M. S. Gottschalk, D. Goulson, A. D. Gove, J. Grogan, M. E. Hanley, T. Hanson, N. R. Hashim, J. E. Hawes, C. Hébert, A. J. Helden, J. A. Henden, L. Hernández, F. Herzog, D. Higuera-Diaz, B. Hilje, F. G. Horgan, R. Horváth, K. Hylander, P. Isaacs-Cubides, M. Ishitani, C. T. Jacobs, V. J. Jaramillo, B. Jauker, M. Jonsell, T. S. Jung, V. Kapoor, V. Kati, E. Katovai, M. Kessler, E. Knop, A. Kolb, Á. Kőrösi, T. Lachat, V. Lantschner, V. Le Féon, G. LeBuhn, J. P. Légaré, S. G. Letcher, N.

A. Littlewood, C. A. López-Quintero, M. Louhaichi, G. L. Lövei, M. E. Lucas-Borja, V. H. Luja, K. Maeto, T. Magura, N. A. Mallari, E. Marin-Spiotta, E. J. Marshall, E. Martínez, M. M. Mayfield, G. Mikusinski, J. C. Milder, J. R. Miller, C. L. Morales, M. N. Muchane, M. Muchane, R. Naidoo, A. Nakamura, S. Naoe, G. Nates-Parra, D. A. Navarrete Gutierrez, E. L. Neuschulz, N. Noreika, O. Norfolk, J. A. Noriega, N. M. Nöske, N. O'Dea, W. Oduro, C. Ofori-Boateng, C. O. Oke, L. M. Osgathorpe, J. Paritsis, A. Parra-H, N. Pelegrin, C. A. Peres, A. S. Persson, T. Petanidou, B. Phalan, T. K. Philips, K. Poveda, E. F. Power, S. J. Presley, V. Proença, M. Quaranta, C. Quintero, N. A. Redpath-Downing, J. L. Reid, Y. T. Reis, D. B. Ribeiro, B. A. Richardson, M. J. Richardson, C. A. Robles, J. Römbke, L. P. Romero-Duque, L. Rosselli, S. J. Rossiter, T. H. Roulston, L. Rousseau, J. P. Sadler, S. Sáfián, R. A. Saldaña-Vázquez, U. Samnegård, C. Schüepp, O. Schweiger, J. L. Sedlock, G. Shahabuddin, D. Sheil, F. A. Silva, E. M. Slade, A. H. Smith-Pardo, N. S. Sodhi, E. J. Somarriba, R. A. Sosa, J. C. Stout, M. J. Struebig, Y. H. Sung, C. G. Threlfall, R. Tonietto, B. Tóthmérész, T. Tscharntke, E. C. Turner, J. M. Tylianakis, A. J. Vanbergen, K. Vassilev, H. A. Verboven, C. H. Vergara, P. M. Vergara, J. Verhulst, T. R. Walker, Y. Wang, J. I. Watling, K. Wells, C. D. Williams, M. R. Willig, J. C. Woinarski, J. H. Wolf, B. A. Woodcock, D. W. Yu, A. S. Zaitsev, B. Collen, R. M. Ewers, G. M. Mace, D. W. Purves, J. P. Scharlemann, A. Purvis, The PREDICTS database: a global database of how local terrestrial biodiversity responds to human impacts. *Ecol. Evol.* **4**, 4701–4735 (2014).

56. T. Newbold, L. N. Hudson, S. L. L. Hill, S. Contu, I. Lysenko, R. A. Senior, L. Börger, D. J. Bennett, A. Choimes, B. Collen, J. Day, A. De Palma, S. Díaz, S. Echeverria-Londoño, M. J. Edgar, A. Feldman, M. Garon, M. L. K. Harrison, T. Alhusseini, D. J. Ingram, Y. Itescu, J. Kattge, V. Kemp, L. Kirkpatrick, M.Kleyer, D. L. P. Correia, C. D. Martin, S. Meiri, M. Novosolov, Y. Pan, H. R. P. Phillips, D. W. Purves, A. Robinson, J. Simpson, S. L. Tuck, E. Weiher, H. J. White, R. M. Ewers, G. M. Mace, J. P. W. Scharlemann, A. Purvis, Global effects of land use on local terrestrial biodiversity. *Nature* **520**, 45–50 (2015).

57. B. Sandel, L. Arge, B. Dalsgaard, R. G. Davies, K. J. Gaston, W. J. Sutherland, J-C. Svenning, The Influence of Late Quaternary Climate-Change Velocity on Species Endemism. *Science* **334**, 660 (2011).

58. A. AghaKouchak, F. Chiang, L. S. Huning, C. A. Love, I. Mallakpour, O. Mazdiyasni, H. Moftakhari, S. M. Papalexiou, E. Ragno, M. Sadegh. Climate extremes and compound hazards in a warming world. *Annu. Rev. Earth Planet. Sci.* **48**, 519–548 (2020).

59. N. S. Diffenbaugh, D. Singh, J. S. Mankin, D. E. Horton, D. L. Swain, D. Touma, A. Charland, Y. Liu, M. Haugen, M. Tsiang, B. Rajaratnam, Quantifying the influence of global warming on unprecedented extreme climate events. *Proc. Natl. Acad. Sci.* **114**, 4881–4886 (2017).

60. A. G. Brooke, M. L. Bell, Heat Waves in the United States: Mortality Risk during Heat Waves and Effect Modification by Heat Wave Characteristics in 43 U.S. Communities. *Environ. Health Perspect.* **119**, 210–218 (2011).

61. D. S. Battisti, R. L. Naylor, Historical warnings of future food insecurity with unprecedented seasonal heat. *Science* **323**, 240–244 (2009).

62. D. Mitchell, C. Heaviside, S. Vardoulakis, C. Huntingford, G. Masato, B. P. Guillod, P. Frumhoff, A. Bowery, D. Wallom, M. Allen, Attributing human mortality during extreme heat waves to anthropogenic climate change. *Environ. Res. Lett.* **11**, 074006 (2016).

63. R. M. B. Harris, L.J. Beaumont, T. R. Vance, C. R. Tozer, T. A. Remenyi, S. E. Perkins-Kirkpatrick, P. J. Mitchell, A. B. Nicotra, S. McGregor, N. R. Andrew, M. Letnic, Biological responses to the press and pulse of climate trends and extreme events. *Nat. Clim. Change* **8**, 579–587 (2018).

64. M. Maron, C. A. McAlpine, J. E. M. Watson, S. Maxwell, P. Barnard, Climate-induced resource bottlenecks exacerbate species vulnerability: a review. *Divers. Distrib.* **21**, 731–743 (2015).

65. P. R. Grant, B. R. Grant, R. B. Huey, M. T. J. Johnson, A. H. Knoll, J. Schmitt, Evolution caused by extreme events. *Philos. Trans. R. Soc. B Biol. Sci.* **372**, 20160146 (2017).

66. V. P. Gutschick, H. BassiriRad, Extreme events as shaping physiology, ecology, and evolution of plants: toward a unified definition and evaluation of their consequences. *New Phytol.* **160**, 21–42 (2003).

67. E. Cremonese, G. Filippa, M. Galvagno, C. Siniscalco, L. Oddi, U. M. di Cella, M. Migliavacca. Heat wave hinders green wave: The impact of climate extreme on the phenology of a mountain grassland. *Agric. For. Meteorol.* **247**, 320–330 (2017).

68. F. A. La Sorte, W. M. Hochachka, A. Farnsworth, A. A. Dhondt, D. Sheldon, The implications of mid-latitude climate extremes for North American migratory bird populations. *Ecosphere* **7**, e01261 (2016).

69. D. Fenner, A. Holtmann, A. Krug, D. Scherer, Heat waves in Berlin and Potsdam, Germany – Long-term trends and comparison of heat wave definitions from 1893 to 2017. *Int. J. Climatol.* **39**, 2422–2437 (2019).

70. T. T. Smith, B. F. Zaitchik, J. M. Gohlke, Heat waves in the United States: definitions, patterns and trends. *Clim. Change* **118**, 811–825 (2013).

71. L. E. McPhillips, H. Chang, M.V. Chester, Y. Depietri, E. Friedman, N.B. Grimm, J. S. Kominoski, T. McPhearson, P. Méndez-Lázaro, E.J. Rosi, J. S. Shiva, Defining Extreme Events: A Cross-Disciplinary Review. *Earths Future* **6**, 441–455 (2018).

72. H. Hersbach, B. Bell, P. Berrisford, G. Biavati, A. Horányi, J. M. Sabater, J. Nicolas, C. Peubey, R. Radu, I. Rozum, D. Schepers, A. Simmons, C. Soci, D. Dee, J-N. Thépaut, ERA5 hourly data on single levels from 1979 to present. Copernicus Climate Change Service (C3S) Climate Data Store (CDS). (Accessed on 2020-10-02), 10.24381/cds.adbb2d47 (2018).

73. H. Hersbach, W. Bell, P. Berrisford, A. Horányi, J. M. Sabater, J. Nicolas, R. Radu, D. Schepers, A. Simmons, C. Soci, D. Dee, Global reanalysis: goodbye ERA-Interim, hello ERA5. *ECMFW Newsletter* **159**, 17–24 Available at doi:10.21957/vf291hehd7 (2019).

74. Hoffmann, L. G. Günther, D. Li, O. Stein, X. Wu, S. Griessbach, Y. Heng, P. Konopka, R. Müller, B. Vogel, J. S. Wright, From ERA-Interim to ERA5: the considerable impact of ECMWF's next-generation reanalysis on Lagrangian transport simulations. *Atmospheric Chem. Phys.* **19**, 3097–3124 (2019).

75. Huang, N. E. Z. Shen, S. R. Long, M. C. Wu, H. H. Shih, Q. Zheng, N.-C. Yen, C. C. Tung, H. H. Liu. The empirical mode decomposition and the Hilbert spectrum for nonlinear and non-stationary time series analysis. *Proc. R. Soc. Lond. Ser. Math. Phys. Eng. Sci.* **454**, 903–995 (1998).

76. Z. Wu, N. E. Huang, S. R. Long, C.-K. Peng, On the trend, detrending, and variability of nonlinear and nonstationary time series. *Proc. Natl. Acad. Sci.* **104**, 14889–14894 (2007).

77. S. Ferrari, F. Cribari-Neto, Beta Regression for Modelling Rates and Proportions. *J. Appl. Stat.* **31**, 799–815 (2004).

78. A. B. Simas, W. Barreto-Souza, A. V. Rocha, Improved estimators for a general class of beta regression models. *Comput. Stat. Data Anal.* **54**, 348–366 (2010).

79. S. L. Pimm, P. Raven, Extinction by numbers. *Nature* **403**, 843-845 (2000).

Acknowledgments: We thank Alison Johnston, Peter Arcese, Steven Cooke and Lenore Fahrig for helpful discussions.

Funding:

Liber Ero Fellowship Program

Natural Science and Engineering Research Council of Canada (NSERC) Discovery Grant 2016-06147

Environment and Climate Change Canada Grant GCXE19S058

Author contributions:

Conceptualization: RS, RB, JOH, ADR, SW, HPP, JRB

Methodology: RS, RB, JOH, ADB, JP, FAL, PRR, PHV, JRB

Investigation: RS

Visualization: RS

Funding acquisition: RS, JRB

Writing – original draft: RS, RB, JRB

Writing – review & editing: RS, RB, JOH, ADB, JP, VT, FAL, PRR, PHV, ADR, SW, HPP, JRB

Competing interests: The authors declare no competing interests.

Data and materials availability: All data, scripts and full results are available on Open Science Framework (OSF) and will be assigned a DOI once the manuscript is in print: https://osf.io/e2fuw/?view_only=46eb2e525daf42d29df318a92762d885

Supplementary Materials

Materials and Methods

Figs. S1 to S9

Tables S1 to S4

References (40 – 79)

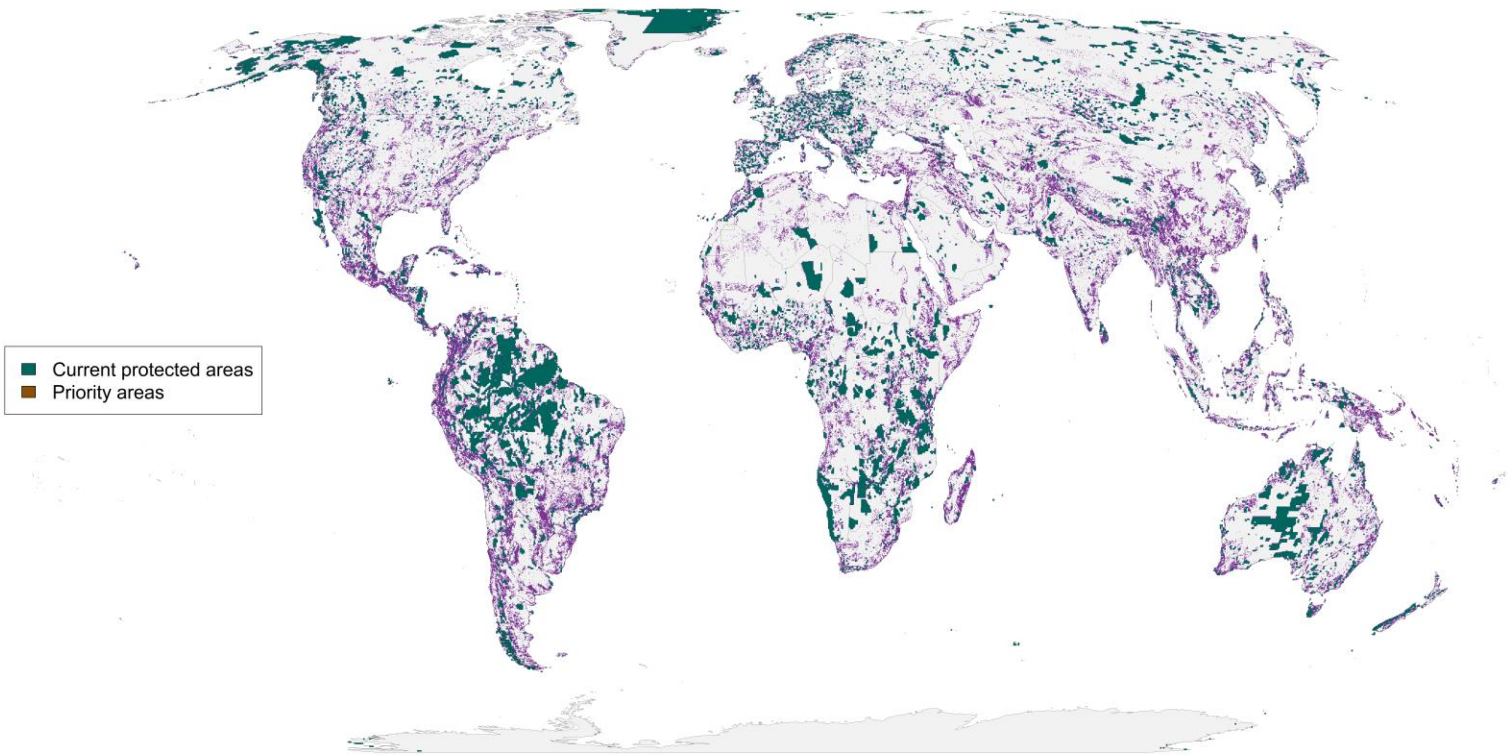

Figure 1: Spatial representation of priority areas for protection to account for governance, land use and climate risk. Accounting for these risks to protected area effectiveness to produce more resilient conservation networks would require 23.5% of land surface to reach suitable habitat protection goals (*26*) for vertebrate species from the IUCN Red List of Threatened Species (*20*).

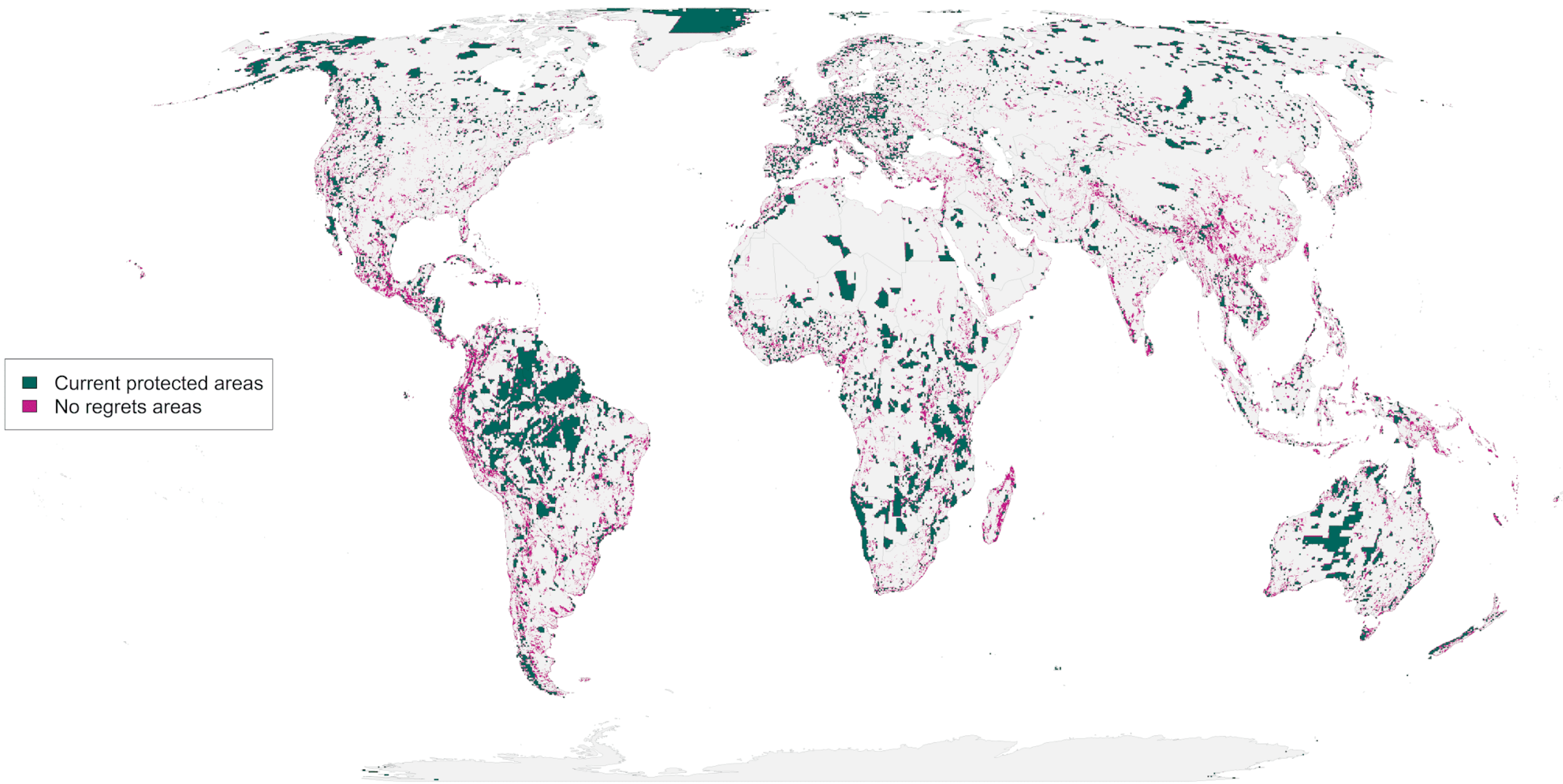

Figure 2: "No regrets" areas comprising 8.5 million km^2 of land that was identified as priority habitat for protection regardless of the risks included in our analysis.

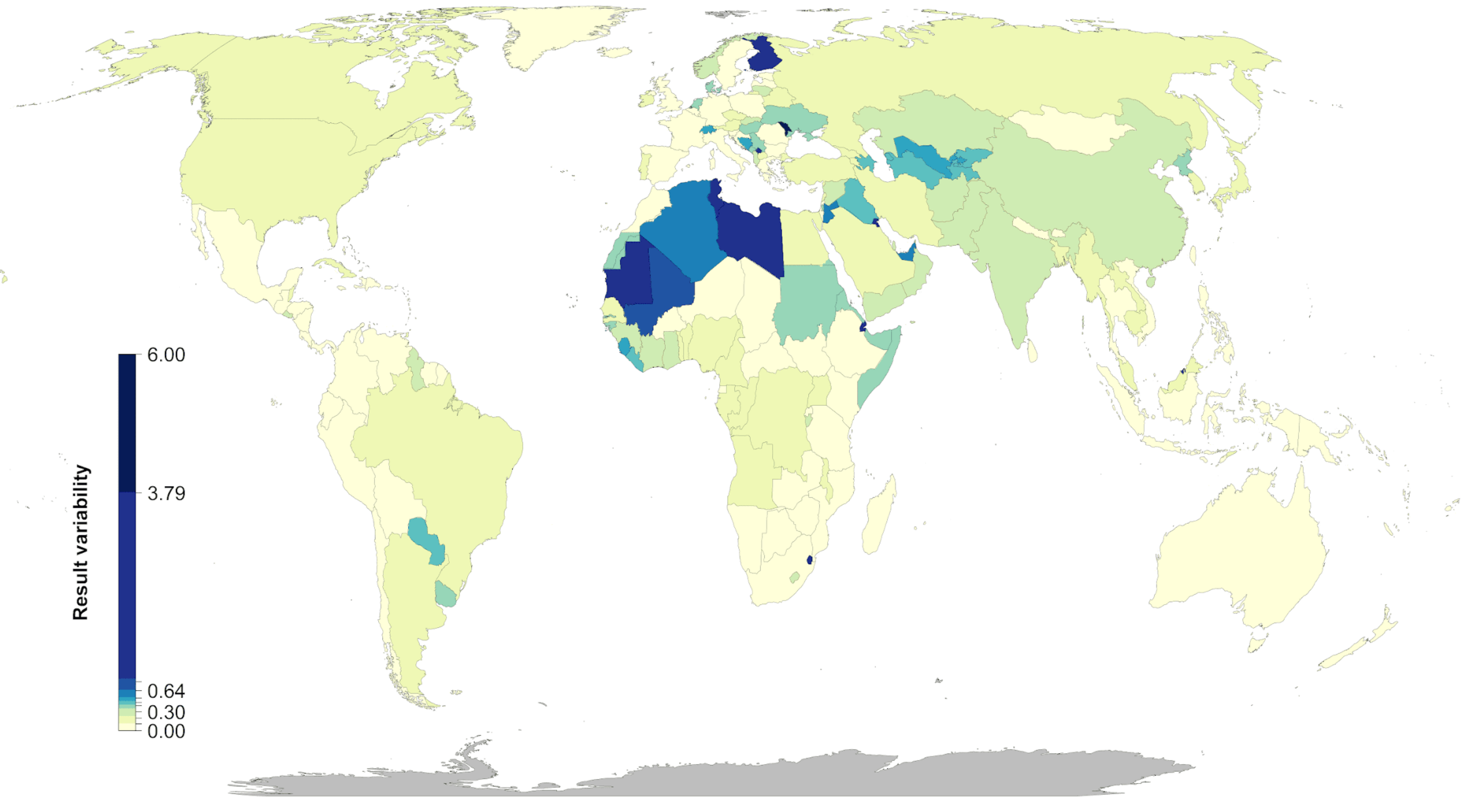

Figure 3: Percent country-level variation between the null scenario and the 15 scenarios including risk. Countries whose results are consistent across the 15 scenarios (e.g., Mexico) have low variation, while countries whose results are less consistent across the 15 scenarios (e.g., Finland) have high variation. The kmeans method (*40*) was used to generate class intervals for visualization.

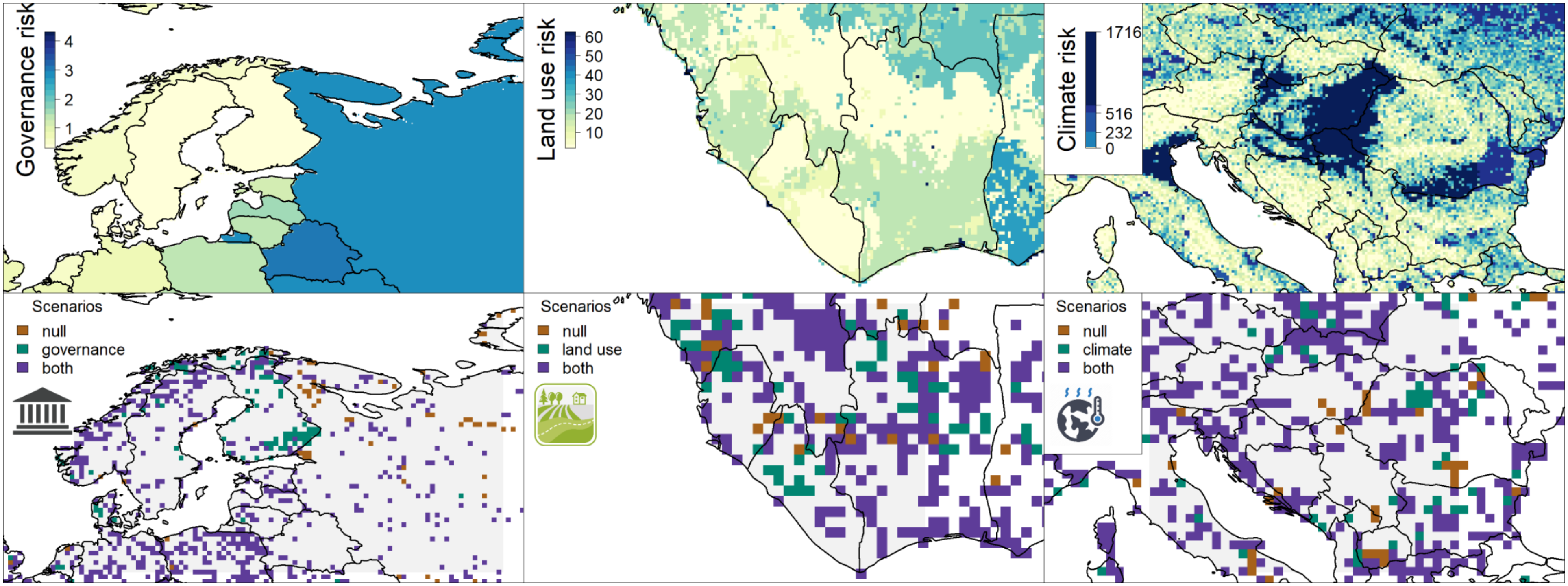

Figure 4: Contrast of using individual risk objectives (governance, land use, climate) to the null scenario of uniform objective structure. The top panels represent the individual risk data for the focal regions. In the bottom panels brown shows null, green the specific risk objective scenario results, and purple where both scenarios agree. The figures show how the spatial configuration of the solutions changes when risk is considered in a scenario. Governance focus is on Finland and Russia, land use risk on Sierra Leone and Liberia, and climate risk on Serbia, Hungary and Kosovo.

Supplementary Materials for

Protected area planning to conserve biodiversity in an uncertain world

Richard Schuster, Rachel Buxton, Jeffrey O. Hanson, Allison D. Binley, Jeremy Pittman, Vivitskaia Tulloch, Frank A. La Sorte, Patrick R. Roehrdanz, Peter H. Verburg, Amanda D. Rodewald, Scott Wilson, Hugh P. Possingham, Joseph R. Bennett

Correspondence to: richard.schuster@glel.carleton.ca

This PDF file includes:

Materials and Methods

Figs. S1 to S9

Tables S1 to S4

Materials and Methods

We used a multi-objective optimization approach that incorporated governance, land use and climate constraints to prioritize the conservation of 29,350 vertebrate species. All scenarios we investigated assumed the current global protected area portfolio is locked in. We further created representation targets for each species on the basis area of habitat maps. Targets for the unpartitioned habitat maps were set following standard practices for global gap analyses and prioritizations (*41*-*43*), except that instead of using the range sizes of species to set the targets, here we used the total extent of suitable habitat for each species following (*26*).

Biodiversity Data

Species AOH ranges were produced for 10,774 species of birds, 5,219 mammals, 4,462 reptiles and 6,254 amphibians with available IUCN range polygon data following the procedure outlined in (*27*). Species range polygons obtained from the IUCN Red List spatial data portal (*44*) and the Birdlife International spatial data zone (*45*) were first filtered for 'extant' range then rasterized to a global 1 km grid in the Eckert IV equal area projection. Individual species range rasters were then modified to only include land cover classes that match the habitat associations for each species. Habitat associations were obtained from the IUCN Red List species habitat classification scheme and were matched to ESA land cover classes for the year 2018 following the crosswalk table presented in (*46*). ESA land cover classification data was aggregated from its native 300 m resolution to match the global 1 km grid using a majority rule. Species ranges were additionally filtered so that only areas within a species accepted elevational range were included. Global elevation data derived from SRTM was obtained from WorldClim v. 2 (*47*). For bird species, seasonal range codes 1-3 (1=year-round; 2=breeding range; 3=non-breeding range) were processed individually and stored as separate range files where applicable.

Basic administrative delineations

National boundaries were derived from the Global Administrative Areas database (*48*). We obtained protected area boundaries from the World Database on Protected Areas (*49*). Following standard procedures for cleaning the protected area dataset (*41,50*), we (i) projected the data to an equal-area coordinate system (World Behrman), (ii) excluded reserves with unknown or proposed designations, (iii) excluded UNESCO Biosphere Reserves (*51*), (iv) buffered sites represented as point localities to their reported area, (v) dissolved boundaries to prevent issues with overlapping areas, and (vi) removed slivers (code available at https://github.com/jeffreyhanson/global-protected-areas). After the protected area data were modified as described above, we overlaid the protected area boundaries with a 10 x 10 km grid covering the Earth. These spatial data procedures were implemented using ArcMap (version 10.3.1) and python (version 2.7.8).

Governance risk

Conservation risk due to governance can affect the outcomes of strategies, and effective governance can promote the resilience of conservation in the face of sociopolitical and economic shocks. We used worldwide governance indicators from the World Bank (*15*) to capture these pressures. The indicators include six scaled measures: voice and accountability; political stability and absence of violence; government effectiveness; regulatory quality; rule of law; and control of corruption (see Table S4 for definitions). We chose these indicators because evidence suggests that they reliably predict protected area effectiveness (*52*) and state investment and efforts for biodiversity conservation (*51*). For each country, we used a mean of annual averages of all six measures (*53*) (Fig. S1).

Land use risk

We used a recently developed global land systems map produced by (*16*) to incorporate the risk of land use change. This map is based on a global land systems map for the year 2000 (*54*) at a 9.25 km^2 spatial resolution but is refined based on recent land-cover and land use datasets to a spatial resolution of 1 km^2. (*16*) further estimated the impact of land use and land use intensity on biodiversity, with data originating from the PREDICTS project (*53*). They first matched their land-systems classes to varying intensity levels for each land use type (for detailed conversion table, see ref (*54*)). This allowed (*16*) to calculate average biodiversity loss per land system (relative to an unimpacted baseline) by taking the mean model estimates of biodiversity loss per land use intensity class from previous work (*55*). The result gives average relative biodiversity gain or loss per land-system class. Here, we used their modelled mean estimates (following (*56*)) of relative percent biodiversity change for each land-system class for species abundance as a measure of the land use pressure (Fig. S2).

<u>Climate risk</u>

Velocity of climate change in an instantaneous measurement of how projected temperature increases translate to horizontal velocity on the landscape (*17*). It is an integration of both the rate of change in average climate and landscape properties that govern how bands of similar temperature redistribute spatially as climate changes. For example, in a region with high topographic diversity, a species may be able to track its climatic niche through relatively small dispersal distances (e.g. 10s or 100s of meters) upslope or downslope. By contrast, keeping pace with preferred climate under the same magnitude of temperature rise in the plains may require much larger dispersal distances – 100s or 1000s of kilometers. The local velocity of climate change, although a purely physical property, has biological relevance when linked with individual species-level dispersal capacity. Velocity of historical climate change since the last glacial maximum has been suggested as a major driver of patterns of species endemism (e.g. (*57*)) and is commonly used as a biologically scaled metric of climate exposure (e.g. (*19*)). Velocity of future temperature change used here follows the method of (*17*) – and is essentially the ratio of the projected temporal rate of change (C/year) to the spatial rate of change (C/km). Projected temporal rate of change is based on the 20 year mean (2040-2060) projection for mean annual temperature from the HadGEM2-ES model (CMIP5) and the baseline (1960-1990) temperature available from Worldclim v1.4. Spatial rate of change was derived from 30 arc second elevation data and calculated with the 'terrain' function from the R 'raster' package.

We also explored an alternative measure of climate risk: exposure to extreme events. Anthropogenic climate change is affecting the frequency and duration of extreme heat events (*58,59*). Exposure to these events can adversely affect human populations (*60-62*) and natural systems (*10,63*). For species in natural systems, these events can further the decline and extirpation of populations, increasing the chances of extinction (*10,64*). Extreme heat events and extreme cold events can also promote the formation of novel ecosystems (*63*), generate enhanced selection pressures (*65,66*), and change the phenology of life history events (*67,68*). There are a number of climate indices that have been used to estimate the occurrence of these events (*69,70*). These indices are often context specific and there is little consensus on the most appropriate technique (*71*).

For this alternative measure, we estimated climatic risk based on the estimated trend in the annual proportion of days containing extreme heat events from 1979 to 2019 (*18*). Extreme heat events were estimated using hourly air temperature at 2 m above the surface and gridded at a 31 km (0.28125° at the equator) spatial resolution (*72*). The temperature data was acquired from the European Centre for Medium-Range Weather Forecasts (ECMWF) fifth generation atmospheric reanalysis of the global climate (ERA5) (*73,74*). The approach first extracted daily minimum and maximum temperature for each grid cell over the 41-year period. To reduce the influence of warming trends, the daily minimum and maximum temperature was then detrended across years for each day and grid cell using empirical mode decomposition (EMD) (*75,76*). The occurrence of extreme heat events was estimated using the following approach: The detrended minimum and maximum temperature data was treated as normally distributed across years for each day and grid cell. The probability density function for the detrended minimum and maximum temperature was then estimated using the mean and standard deviation calculated across years for each day and grid cell. Extreme heat events occurred when the probabilities for both minimum and maximum temperature on a given day and grid cell were within the 0.95-1.00 quartile of the probability density function. The trend in the annual proportion of days containing extreme heat events for each year was calculated for each grid cell using beta regression with a logit link function and an identity function in the precision model (*77,78*) (Fig. S7 – S9). See (*18*) for additional details.

Multi-objective optimization of pressure reduction

We processed all data described previously to a 10 x 10 km resolution and clipped data to the extent of land based on the global administrative areas database. We then developed an extension on the minimum set problem, which has the goal to identify a set of sites within a planning area that represents all conservation targets in the fewest number of sites (*22*). Instead of including a single objective in the problem formulation, we expanded it to include multiple objectives. Specifically, we used a hierarchical (lexicographic) approach that assigns a priority to each objective, and sequentially optimizes for the objectives in order of decreasing priority. At each step, it finds the best solution for the current objective, but only from among those that would not degrade the solution quality for higher-priority objectives. We considered up to three objectives in our prioritization scenarios, i) governance risk, ii) land use risk, and iii) climate risk. To compare different scenarios, we calculated solutions for each unique objective combination (n = 15), as well as one where we use a constant objective function as the null scenario, as the order of the hierarchy can influence the results.

In systematic conservation planning, conservation features describe the biodiversity units (e.g., species, communities, habitat types) that are used to inform protected area establishment. Planning units describe the candidate areas for protected area establishment (e.g., cadastral units). Each planning unit contains an amount of each feature (e.g., presence/absence, number of individuals). A prioritization describes a candidate set of planning units selected for protected establishment. Each feature has a representation target indicating the minimum amount of each feature that ideally should be held in the prioritization (e.g., 50 presences, 200 individuals). To minimize risk, we have a set of datasets describing the relative risk associated with selecting each planning unit for protected area establishment. Thus, we wish to identify a prioritization that meets the representation targets for all of the conservation features, with minimal risk.

Let I denote the set of conservation features (indexed by i), and J denote the set of planning units (indexed by j). To describe existing conservation efforts, let p_j indicate (i.e., using zeros and ones) if each planning unit $j \in J$ is already part of the global protected area system. To describe the spatial distribution of the features, let A_{ij} denote (i.e., using zeros and ones) if each feature is present or absent from each planning unit. To ensure the features are adequately represented by the solution, let t_i denote the conservation target for each feature $i \in I$. Next, let D denote the set of risk datasets (indexed by d). To describe the relative risk associated with each planning unit, let R_{dj} denote the risk for planning units $j \in J$ according to risk datasets $d \in D$.

$$x_j = \begin{cases} 1, & \text{if } j \text{ selected for prioritisation,} \\ 0, & \text{else} \end{cases} \qquad \text{(eqn 1a)}$$

The problem contains the binary decision variables x_j for planning units $j \in J$.

The reserve selection problem is formulated following:

$$\operatorname{lexmin}\ f_1(x), f_2(x), \ldots f_D(x) \qquad \text{(eqn 2a)}$$

$$\text{subject to } f_d(x) = \sum_{j \in J} R_{dj} x_j \qquad \forall d \in D \qquad \text{(eqn 2b)}$$

$$\sum_{j \in J} A_{ij} \geq t_i \qquad \forall i \in I \qquad \text{(eqn 2c)}$$

$$x_j \geq p_j \qquad \forall j \in J \qquad \text{(eqn2d)}$$

$$x_j \in \{0, 1\} \qquad \forall j \in J \qquad \text{(eqn 2e)}$$

The objective function (eqn 2a) is to hierarchically (lexicographically) minimize multiple functions. Constraints (eqn 2b) define each of these functions as the total risk encompassed by selected planning units given each risk dataset. Constraints (eqn 2c) ensure that the representation targets (t_i) are met for all features. Constraints (eqn 2d) ensure that the existing protected areas are selected in the solution. Finally, constraints (eqns 2e) ensure that the decision variables x_j contain zeros or ones.

For all scenarios we locked in current protected areas. Following (*26*), we used flexible targets for suitable habitat based on species' ranges. Species with less than 1,000 km^2 of suitable habitat were assigned a 100% target (1,802 amphibians, 893 avian and 645 mammalian species), species with more than 250,000 km2 of suitable habitat were assigned a 10% target (712 amphibians, 4,518 avian and 1,868 mammalian species) and species with an intermediate amount of suitable habitat were assigned a target by log-linearly interpolating values between the previous two thresholds (2,683 amphibians, 5,190 avian and 2,557 mammalian species). Migratory bird species were assigned targets for each seasonal distribution separately). Additionally, to prevent species with very large suitable habitats from requiring excessively large amounts of area to be protected, the targets for species' distributions larger than 10,000,000 km^2 were capped at 1,000,000 km^2. This upper limit affected only 206 (1%) species, and sensitivity analyses showed that it had little effect on our results. We acknowledge that these targets are arbitrary; however, they are more precise than previous targets based on species' ranges (which can contain a large amount of unsuitable habitat), and accounts for the increased vulnerability of species with smaller range sizes (*79*), as well as the difficulty in conserving all habitat for species that occur over large areas.

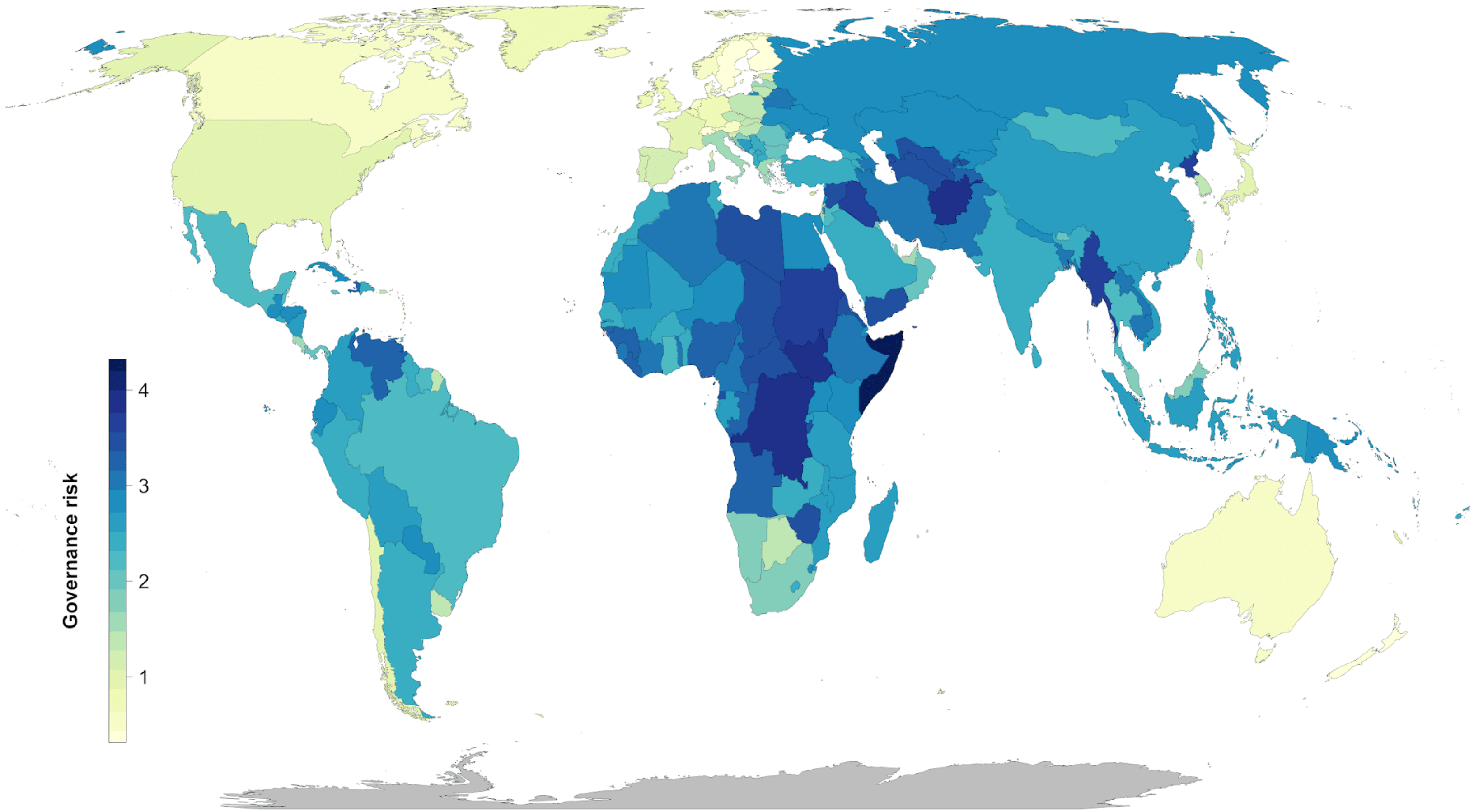

Fig. S1. Governance risk (yellow = low, blue= high)

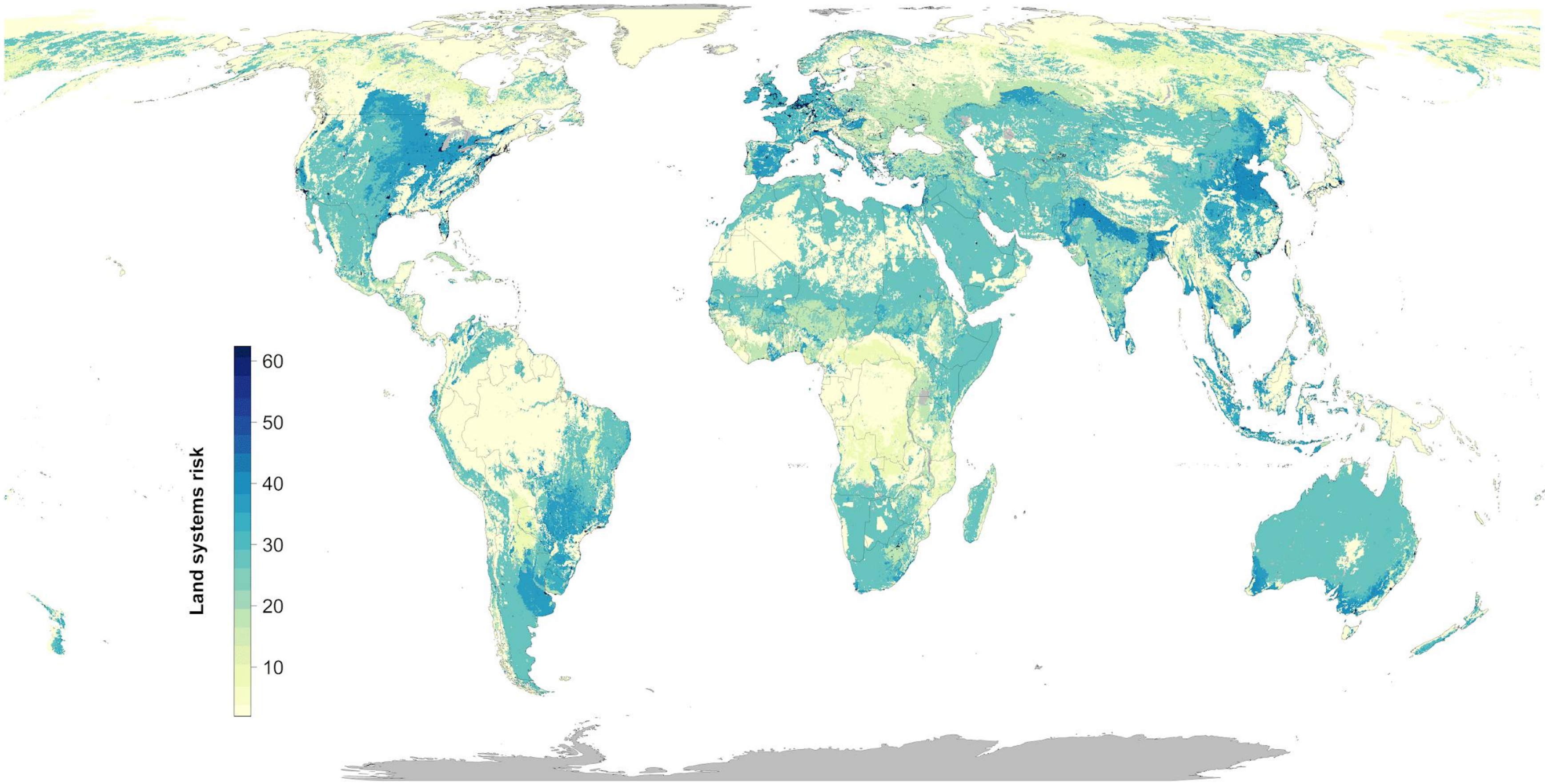

Fig. S2. Land systems risk (yellow = low, blue= high)

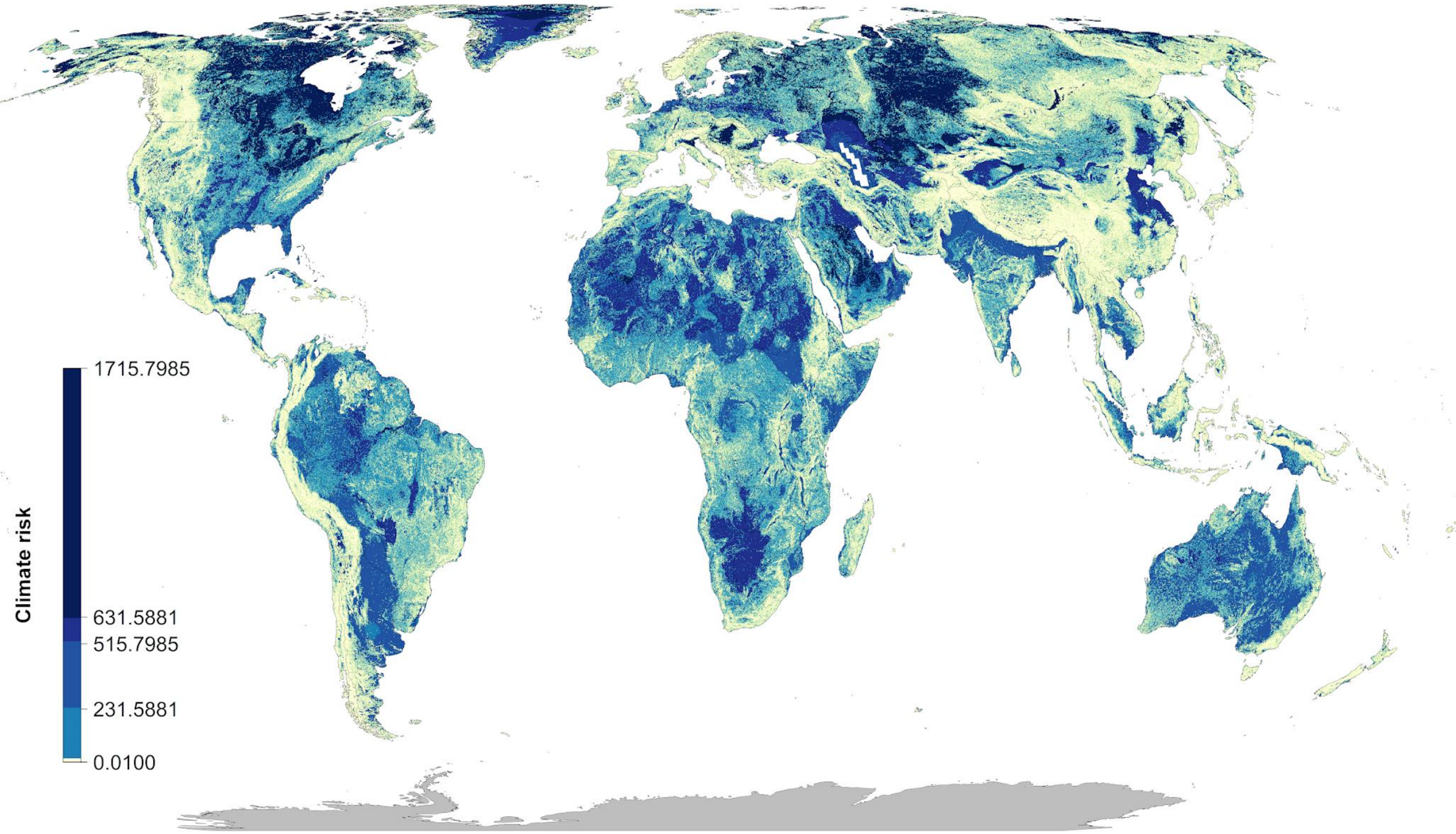

Fig. S3. Climate risk (climate velocity) (yellow = low, blue= high)

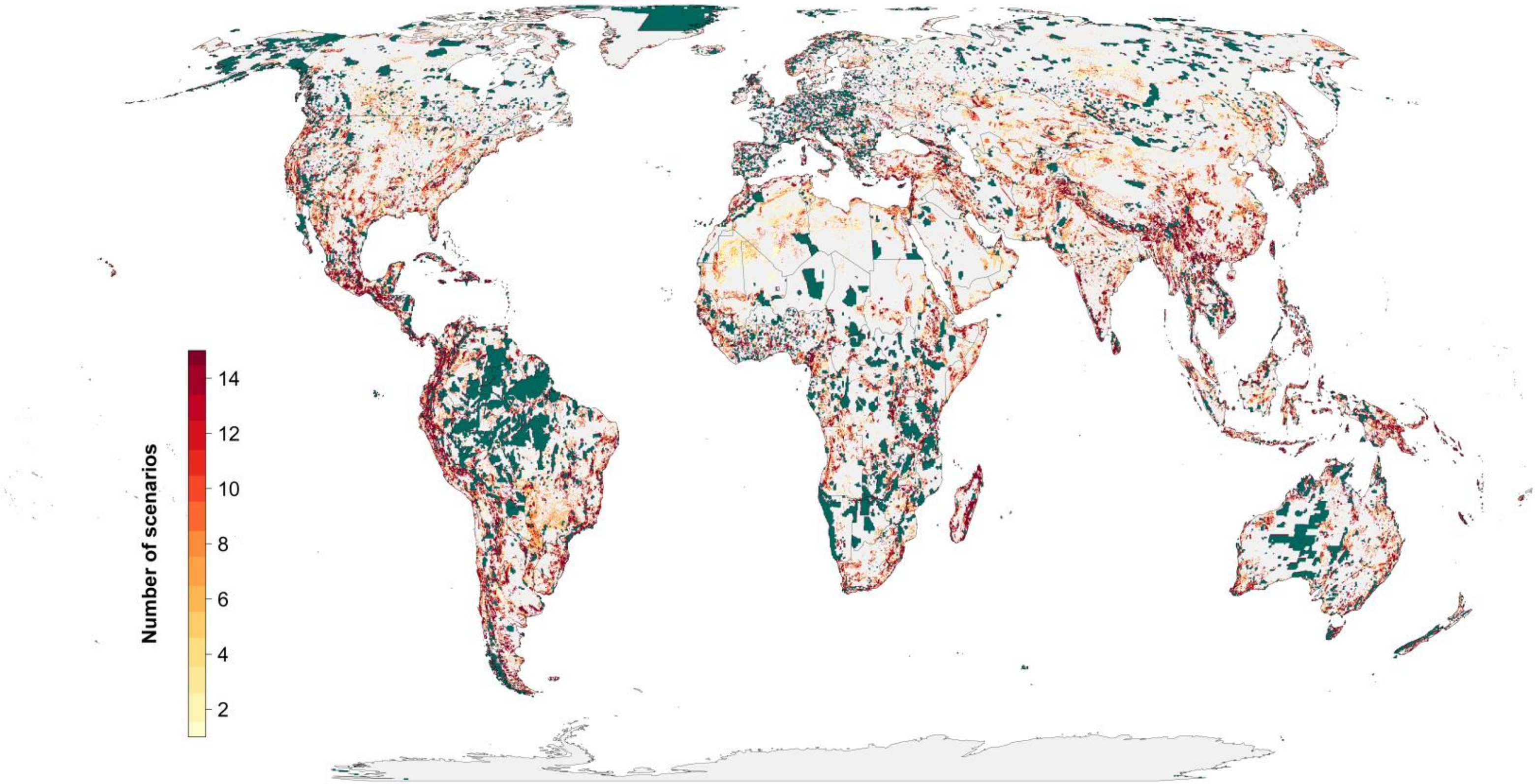

Fig. S4: Scenario overlap. green = protected areas. Color gradient from yellow (one scenario) to red (15 scenarios) = overlap.

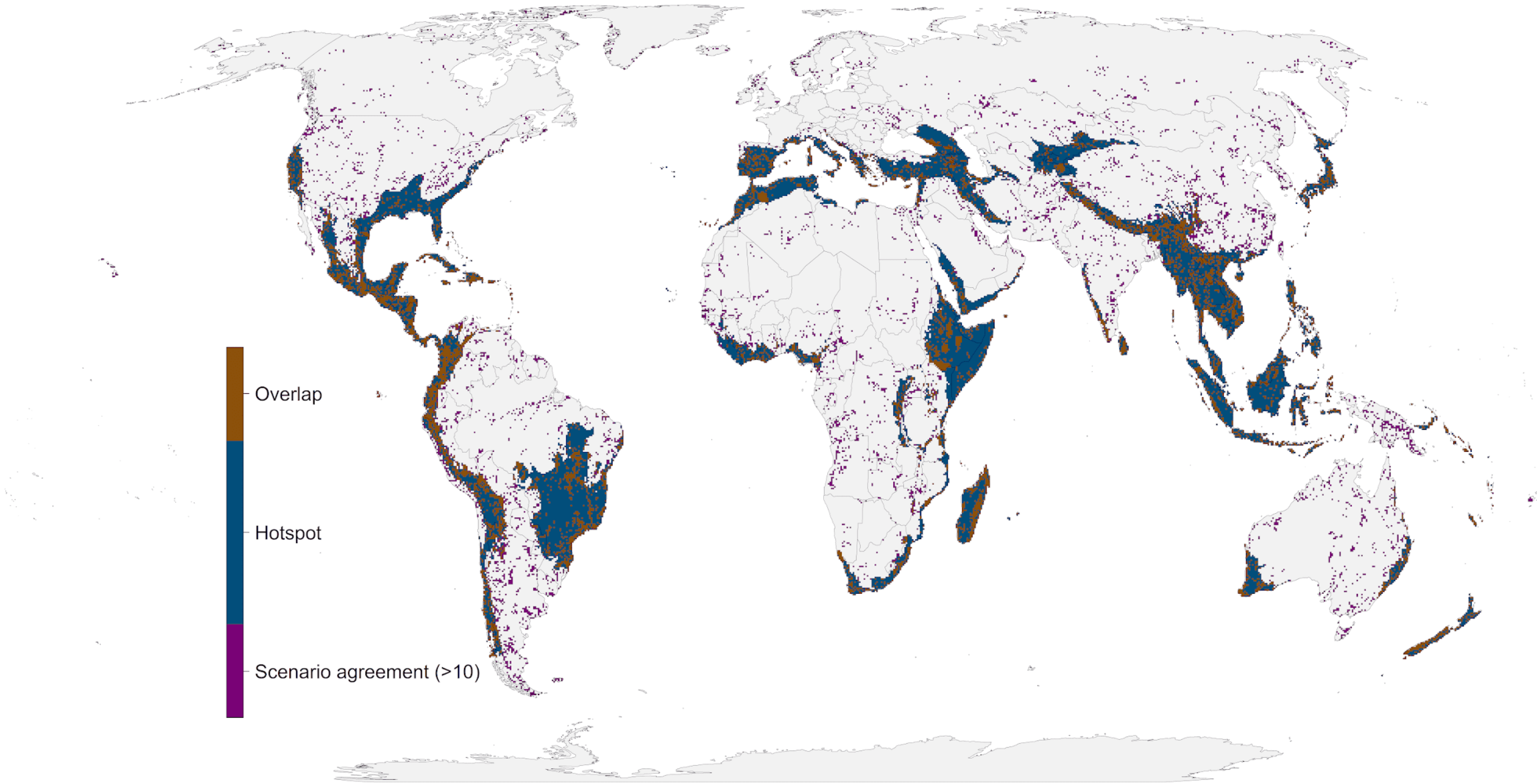

Fig. S5. Areas of high scenario overlap (>10 scenarios, green) compared to biodiversity hotspots (*28*) (blue).

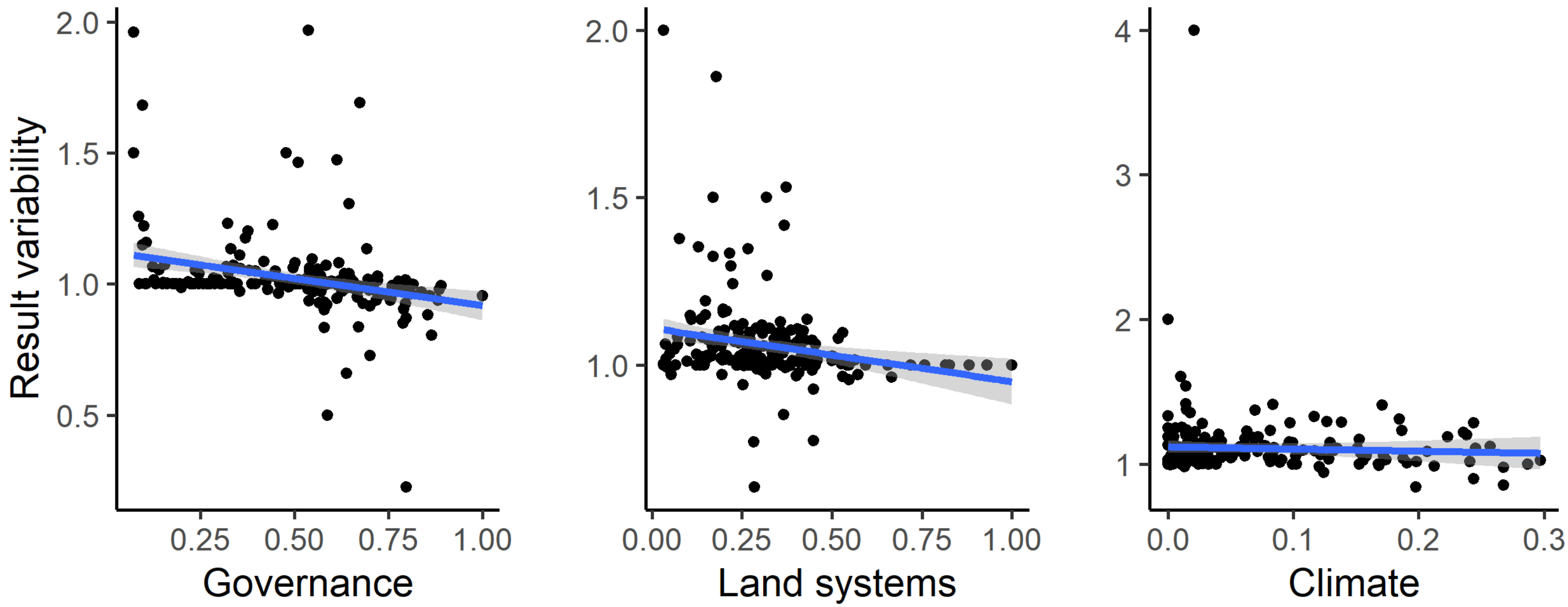

Fig. S6: Influence of average country specific risk factors on the optimization outcomes compared between null scenario and the scenarios including one of the risk factors. Each data point represents the results for one country. The fitted blue lines and 95% confidence bands are from ordinary least-squares regression.

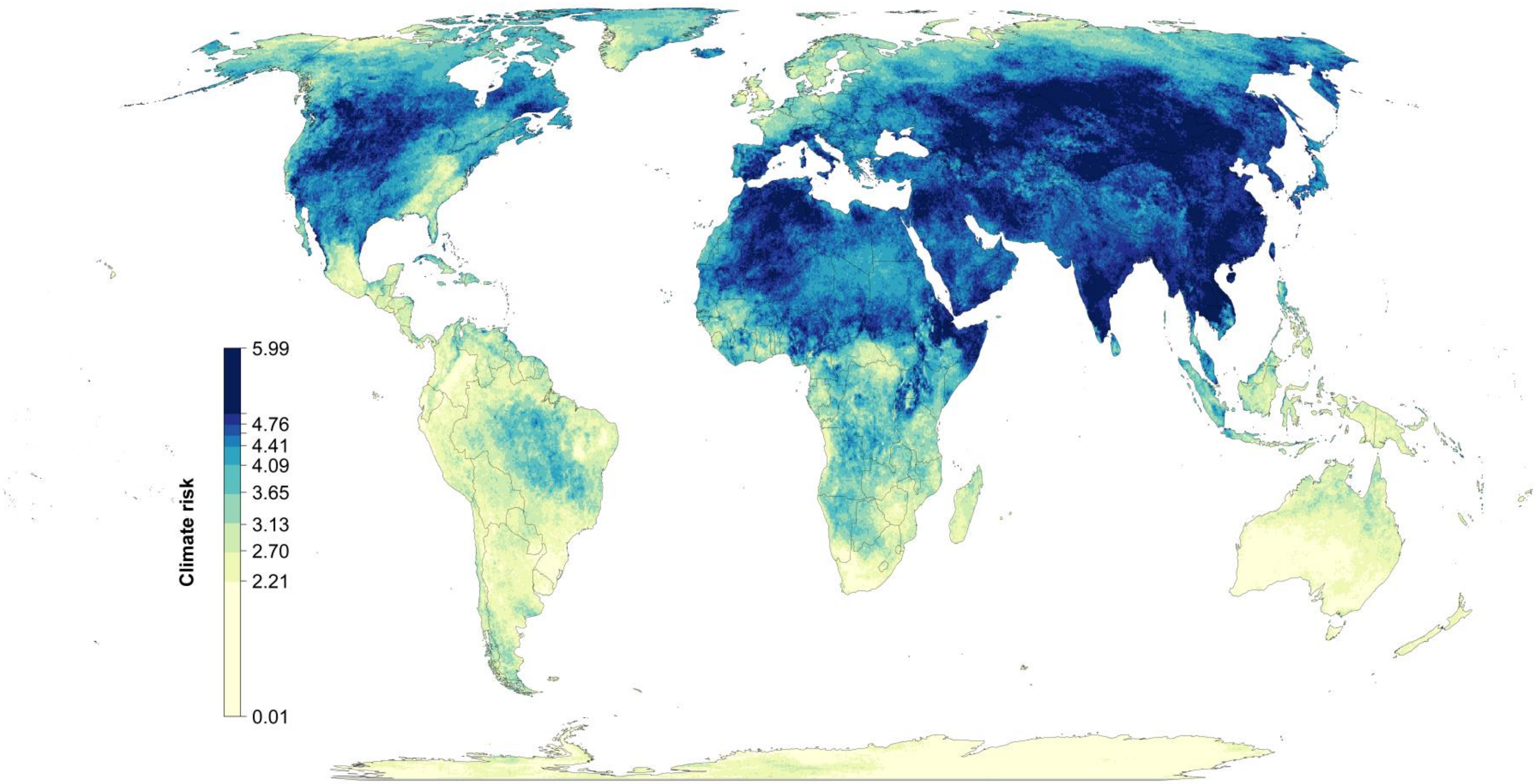

Fig. S7. Alternative climate risk metric (extreme heat events) (yellow = low, blue= high)

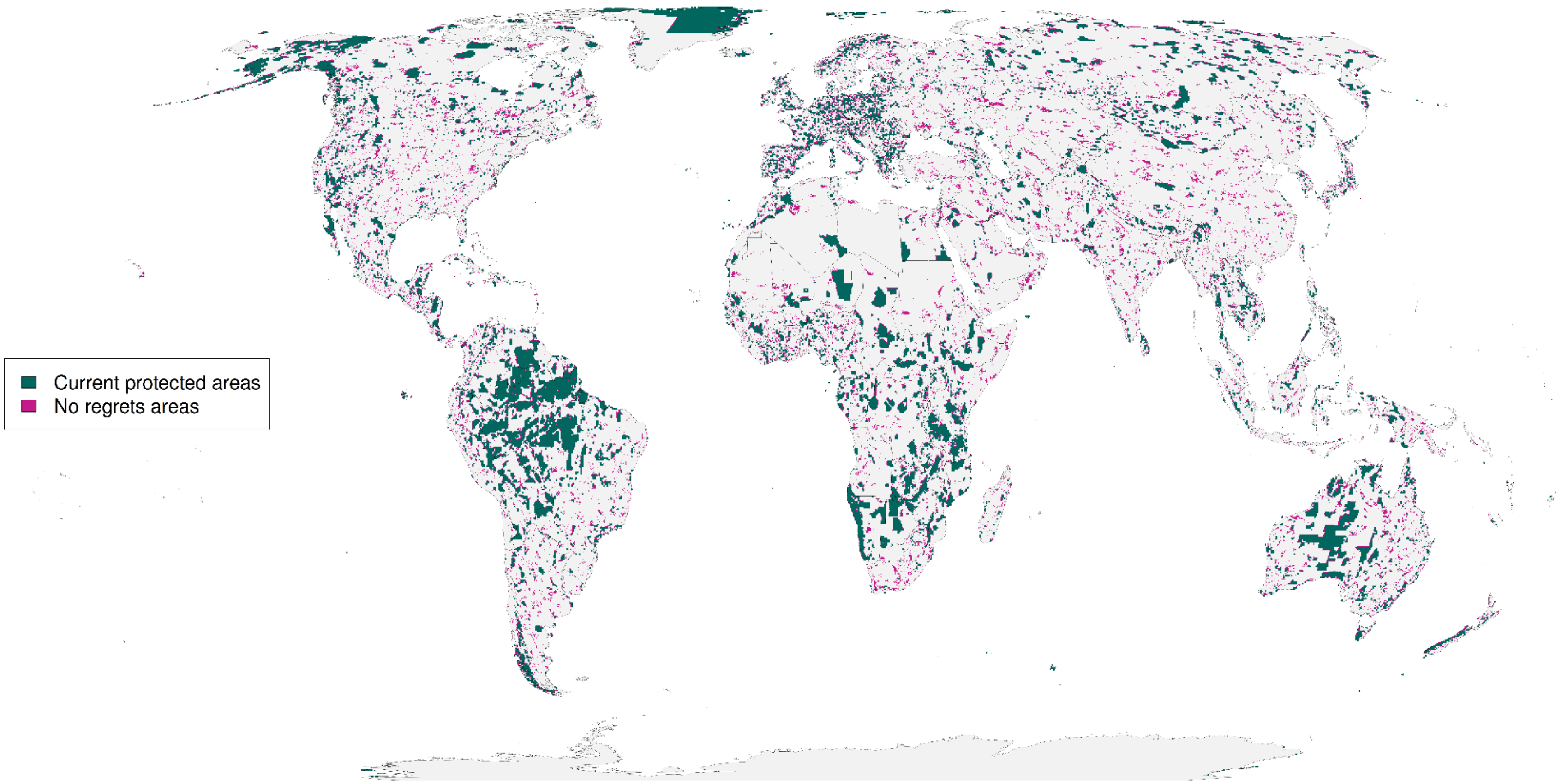

Fig. S8: Alternative climate risk scenario "No regrets" areas that were identified as priority habitat for protection regardless of the risks included in our analysis.

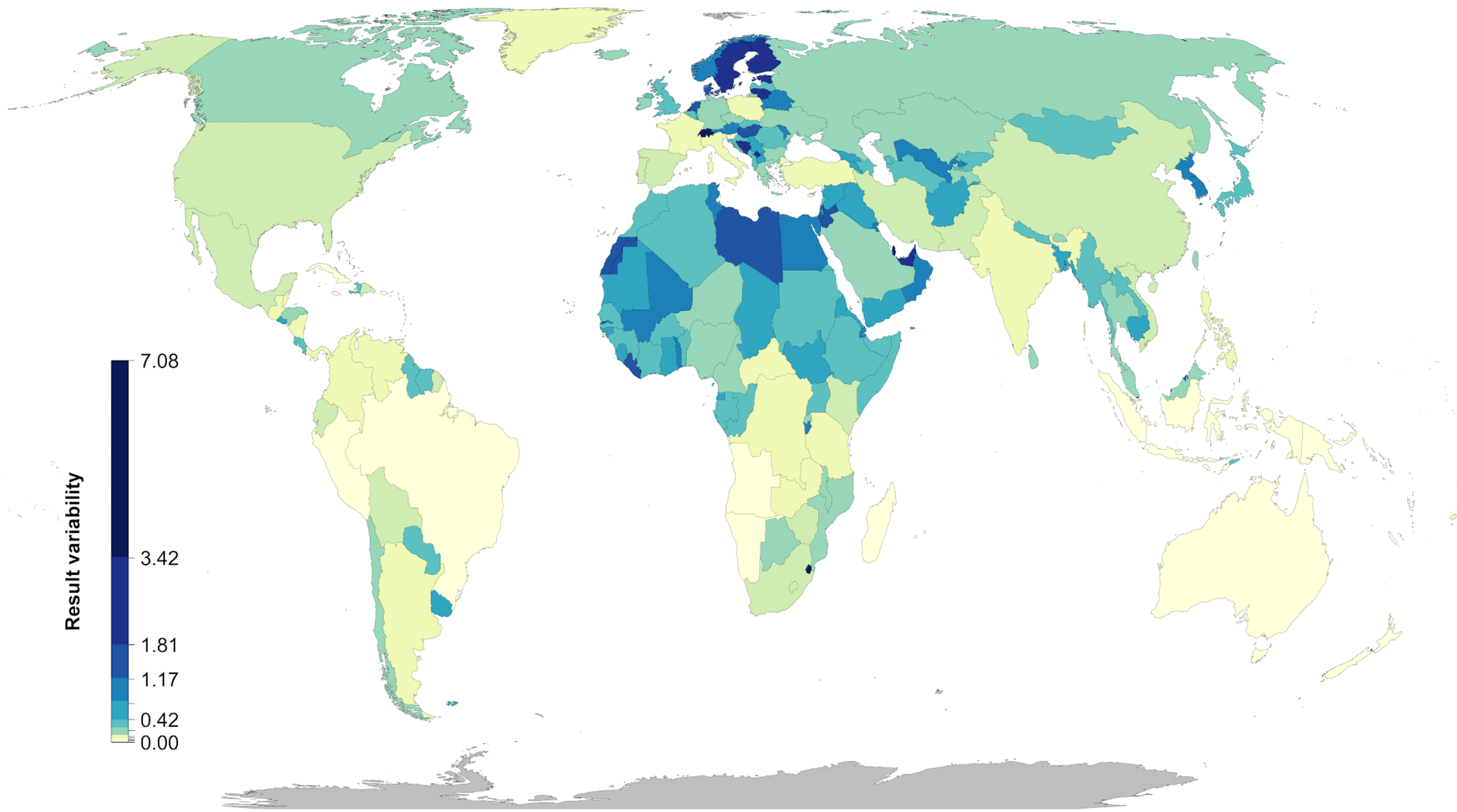

Fig. S9: Alternative climate risk scenarios percent country-level variation between the null scenario and the 15 scenarios including risk. Countries whose results are consistent across the 15 scenarios (e.g., Brazil) have low variation, while countries whose results are less consistent across the 15 scenarios (e.g., Sweden) have high variation. The kmeans method (*37*) was used to generate class intervals for visualization.

Scenario	Risk factors included	Global land area protected [%]
null	-	21.27
1	G	21.35
2	L	22.31
3	C	23.79
4	G > L	21.93
5	L > G	22.18
6	G > C	23.78
7	C > G	23.31
8	L > C	23.52
9	C > L	22.99
10	G > L > C	23.52
11	G > C > L	23
12	L > G > C	23.5
13	L > C > G	23.08
14	C > G > L	22.3
15	C > L > G	22.99

Table S1. Scenarios explored and global protection results. The risk factor order represents the order risk factors were included in the hierarchical prioritization. (G = governance, L = land use, C = Climate).

	Afghanistan	Åland	Albania	Algeria
N	15.95	57.14	38.46	10.62
G	14.95	85.71	35.66	7.71
L	17.03	85.71	43.71	10.32
C	19.25	57.14	46.15	13.69
GL	15.87	85.71	37.41	8.94
LG	16.55	100	38.11	11.59
GC	19.3	57.14	46.5	13.71
CG	17.89	71.43	39.16	12.74
LC	17.8	71.43	44.06	13.07
CL	19.52	57.14	40.56	13.36
GLC	17.8	57.14	43.71	13.15
GCL	19.44	57.14	41.96	13.38
LGC	17.81	57.14	44.06	13.05
LCG	16.58	85.71	38.11	12.36
CGL	17.52	85.71	43.36	12.4
CLG	19.52	57.14	40.56	13.36

Table S2. Country specific results for the 15 scenarios investigated. Numbers represent % of land area of a country selected (including existing protected areas).
(As an example 5 countries included here, full list in csv. N = null, G = governance, L = land use, C = Climate)
https://drive.google.com/file/d/1eD4y4K8XG4nxnRL5fNtiTqzuqfIJ_DfB/view?usp=sharing

Country.Name	Country.Code	MeanIndex	SDIndex
Afghanistan	AFG	-1.65038	0.16074
Albania	ALB	-0.28043	0.219515
Algeria	DZA	-0.86838	0.121774
American Samoa	ASM	0.747997	0.127264
Andorra	AND	1.359029	0.04054
Angola	AGO	-1.16429	0.217384
Anguilla	AIA	1.138708	0.225908
Antigua and Barbuda	ATG	0.687351	0.143042
Argentina	ARG	-0.19472	0.196541
Armenia	ARM	-0.29545	0.091655
Aruba	ABW	1.181311	0.090913
Australia	AUS	1.591282	0.033469
Austria	AUT	1.559385	0.080972
Azerbaijan	AZE	-0.84662	0.123512
Bahamas, The	BHS	0.991142	0.212122
Bahrain	BHR	0.067606	0.189151
Bangladesh	BGD	-0.8678	0.131258
Barbados	BRB	1.154432	0.145899

Table S3. Governance risk score table (see csv)
(As an example Afghanistan – Barbados are included below)
https://drive.google.com/file/d/1g_LePBfCbphXzTiCOXCzQtNLSSYoV6me/view?usp=sharing

Indicator	Definition
	Source: World Bank, 2020 (https://datacatalog.worldbank.org/dataset/worldwide-governance-indicators)
Voice and accountability	“Voice and accountability captures perceptions of the extent to which a country's citizens are able to participate in selecting their government, as well as freedom of expression, freedom of association, and a free media.”
Political stability and absence of violence	“Political Stability and Absence of Violence/Terrorism measures perceptions of the likelihood of political instability and/or politically-motivated violence, including terrorism.”
Government effectiveness	“Government effectiveness captures perceptions of the quality of public services, the quality of the civil service and the degree of its independence from political pressures, the quality of policy formulation and implementation, and the credibility of the government's commitment to such policies.”
Regulatory quality	“Regulatory quality captures perceptions of the ability of the government to formulate and implement sound policies and regulations that permit and promote private sector development.”
Rule of law	“Rule of law captures perceptions of the extent to which agents have confidence in and abide by the rules of society, and in particular the quality of contract enforcement, property rights, the police, and the courts, as well as the likelihood of crime and violence.”
Control of corruption	“Control of corruption captures perceptions of the extent to which public power is exercised for private gain, including both petty and grand forms of corruption, as well as "capture" of the state by elites and private interests.”

Table S4. Worldwide governance indicator definitions from the World Bank (15).